

# Application of the pushover method to the Warth bridge

**Vivier Aurélie, Project engineer**

Systra, 3 avenue du Coq, 75009 Paris, [avivier@systra.com](mailto:avivier@systra.com), +33140187991

**Sekkat Dayae, Project engineer**

Systra, 3 avenue du Coq, 75009 Paris, [dsekkat@systra.com](mailto:dsekkat@systra.com)

**Montens Serge, Director of Civil and Structural Department**

Systra, 3 avenue du Coq, 75009 Paris, [smontens@systra.com](mailto:smontens@systra.com)



## SUMMARY:

The Warth bridge was constructed in the 70's in Austria. It is composed of seven spans of a box girder with six hollow core piers. In order to evaluate seismic capacity of the bridge, a pushover analysis was performed. The pushover method is the one developed in the Eurocode 8 adapted for having damage curves (according to the French Setra guide "Seismic diagnosis and retrofit of existing bridges"). The analysis was done with a hand calculation and with the Sofistik software in order to compare the results. This analysis is interesting because it brings to light the high capacity of hollow core bridge piers, and consequently of the bridge, and it allows testing the Eurocode 8 pushover analysis and its limits.

*Key-words: pushover analysis, Warth bridge, Eurocode 8, hollow core bridge piers*

## 1. INTRODUCTION

Using the example of the Warth bridge, the pushover analysis method was developed with a hand calculation and on the software Sofistik. This analysis permitted to validate the principle of modelisation, and to develop the whole method step by step to better understand the behavior of the bridge. This way of calculation put in light some problems of modelisation, and limits of the Eurocode 8. In this article, we will first develop the constitutive laws of materials, taking into account non-conform detailing. Then, we will develop the pushover analysis, with moment-curvature curves, force-displacement curves and then damages curves of the whole bridge.

## 2. DESCRIPTION OF THE BRIDGE

The Warth bridge is located in Austria, on the A2 highway, at 63 km in the south of Vienna. the bridge was built in the 70's for a horizontal acceleration of 0.04g. The bridge is composed of two identical viaducts of 459m, with five spans of 67m and two extreme spans of 62m.

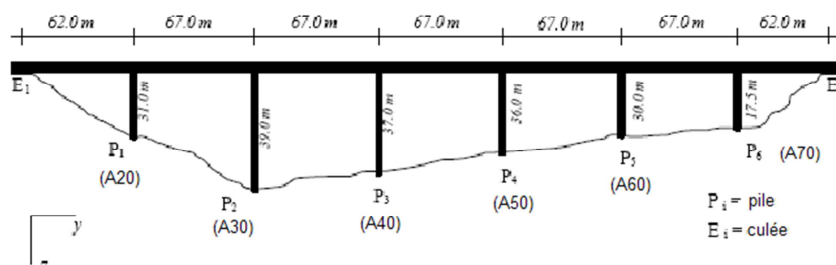


**Figure 1.** Elevation of the Warth bridge

The deck is composed of a continuous box girder prestressed by post-tensioning. For calculation, an axial force of 19MN is considered as dead load on each pier top. The deck is linked to piers by two circular elastomeric bearings of 1.33m<sup>2</sup> of surface and 0.25m of height. The elastomeric bearings are supposed free in all piers and abutments.

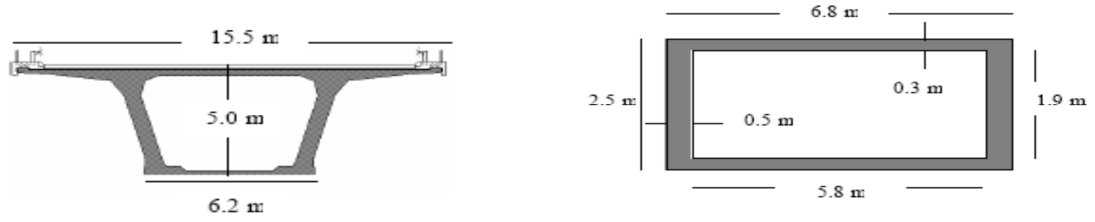


**Figure 2.** Section of the box girder and piers

The Warth bridge piers are hollow core bridge piers of 6.8m \* 2.5m with a hollow core of 5.8m \* 1.9m, that is to say a thickness of walls of 0.5m and 0.3m. Piers height varies from 17.5m to 39m. For all piers, three areas of reinforcement are placed along the pier height. High level of reinforcement is put in place at the bottom and reduced level in the center and the top. Transverse reinforcements are spaced any 200mm along the pier, and are composed of one hook on each wall of the section. Those hooks are 8mm diameter in current sections and 12mm diameter in the bottom of the pier.

### 3. MATERIALS

Characteristics of materials are described in the following table.

**Table 3.1.** Materials characteristics

Concrete		Reinforcement	
f <sub>cm</sub>	43 MPa	f <sub>sy</sub>	545 MPa
f <sub>tm</sub>	3.1 MPa	E <sub>su</sub>	200000 MPa
E <sub>cm</sub>	35000 MPa	ε <sub>su</sub>	0.1

As the anti-seismic details are not in accordance with Eurocode 8 prescriptions for new bridges, material constitutive laws shall be adapted to take into account phenomenon that result from those non adapted details. In the Warth bridge case, three phenomenon have been taken into account: confined concrete, buckling of longitudinal reinforcement and insufficient lap splices.

#### 3.1. Confinement of concrete

In order to modelize confinement of concrete, the model of Mander (J.B. Mander, M.J.N. Priestley and R. Park, *Theoretical stress-strain model for confined concrete*, Journal of structural engineering V.114 No.8, 1988) has been used, according to the appendix E of Eurocode 8-2. For the Warth bridge, the only parameter that influenced the confined concrete law is the density of transverse reinforcement, which is 0.006% at the center of the pier and 0.12% at the top and bottom. We obtained the following laws.

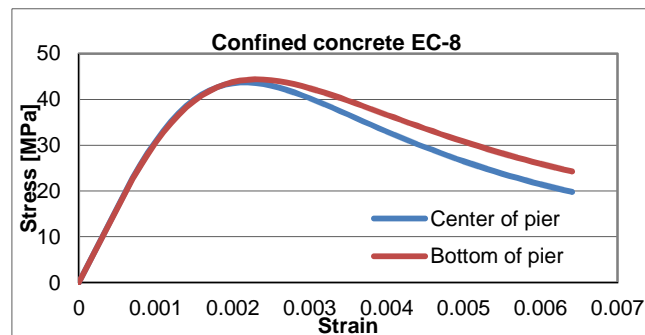


**Figure 3.** Constitutive law for confined concrete

#### 3.2. Steel reinforcement constitutive law

For an existing bridge, as the Warth bridge, the constitutive law of reinforcement shall take into account the lack of transverse reinforcement, which can lead to a premature buckling of longitudinal reinforcement. This phenomenon can be taken into account by the “Gomes and Appleton” model (Augusto Gomes & Julio Appleton, *Nonlinear cyclic stress-strain relationship of reinforcing bars including buckling*, Engineering structure) for buckling between two transversal reinforcements. The reduction of capacity of the longitudinal reinforcement can be estimated considering the articulation of the longitudinal reinforcement between two transversal reinforcements:

$$\sigma_s = \frac{2\sqrt{2}M_p}{A_s s} \times \frac{1}{\sqrt{\varepsilon_s}} \quad (3.1)$$

$A_s$  : area of the longitudinal reinforcement bar,  $M_p$ : Plastic moment of the bar ;  $M_p=0.424\pi R^3 f_y$ ,  $s$  : spacing of transversal reinforcement,  $\varepsilon_s$ : strain of the bar,  $f_y$  : yield strength of the longitudinal reinforcements,  $R$  : radius of longitudinal reinforcement

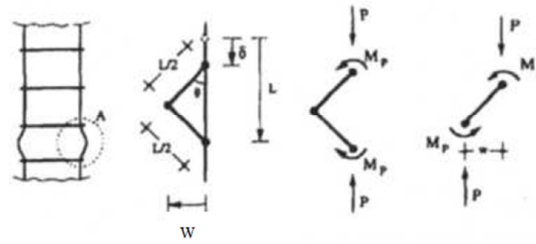


**Figure 4.** Buckling principle between two layers of reinforcement (Gomes and Appleton)

For buckling under several transversal reinforcement layers, the Gomes and Appleton model have been adapted in the Setra guideline “*Diagnostic et renforcement sismiques des ponts existants*”, as following:

$$\sigma_s = 1.5 \frac{(A_t/s_t)_{\text{présent}}}{(A_t/s_t)_{\text{nécessary}}} \frac{2\sqrt{2}M_p}{A_s s} \times \frac{1}{\sqrt{\varepsilon_s}} \quad (3.2)$$

With

$$\left(\frac{A_t}{s_t}\right)_{\text{nécessary}} = \frac{\Sigma A_L f_{ys}}{1.6 f_{yt}} \quad (3.3)$$

$\Sigma A_L$ : sections of longitudinal rebars maintained by hooks (mm<sup>2</sup>),  $f_{yt}$  : yield strength of the ties,  $f_{ys}$  : yield strength of the longitudinal rebars,  $A_t$  : section of one tie,  $s_t$  : distance between ties.

For the Warth bridge, this leads to the following constitutive law (20mm diameter longitudinal rebars)

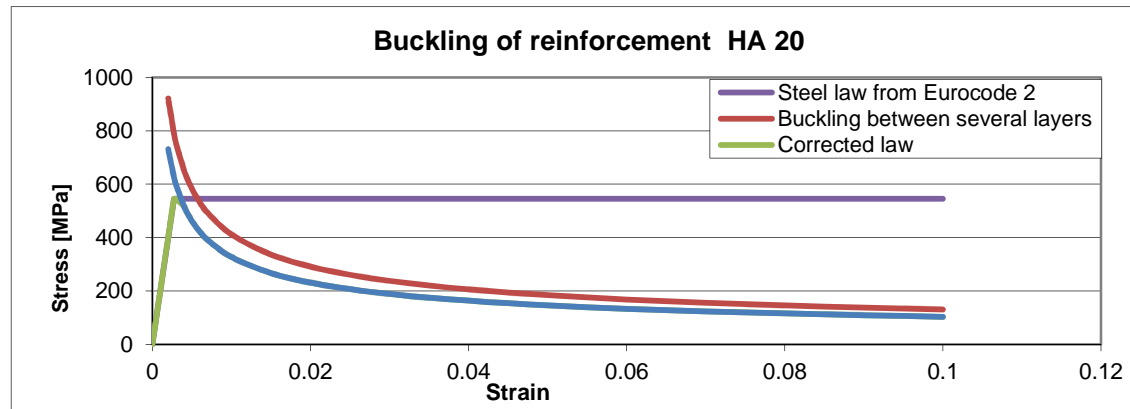


**Figure 5.** Constitutive law for steel reinforcement, 20mm diameter in compression

As the previous curves for constitutive laws are very unfavorable, we considered that ultimate capacity of reinforcement in compression is reached when 20 % of capacity has been lost.

For tension in steel reinforcement, the following law is considered. In this case, oligocyclic fatigue is

not considered in reinforcement. The ultimate limit at 0.1 of deformation is supposed to cover the phenomenon.

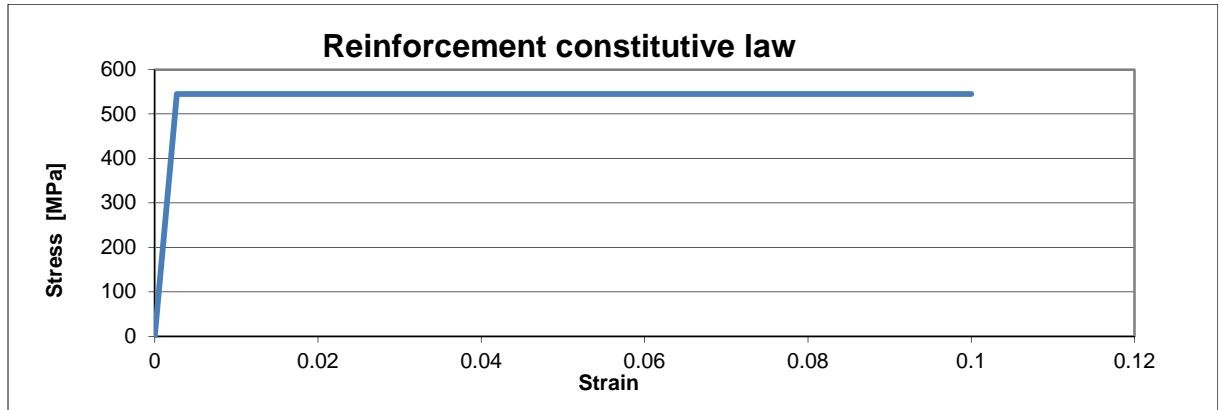


**Figure 6.** Constitutive law for reinforcement in tension

### 3.3. Lap splices

The lap splices length is verified according to the model of Xiao et al (Y. Xiao, R. Ma (1997), *Seismic retrofit of RC circular columns using prefabricated composite jacketing*, Journal of structural engineering, March 1998). We verified that lap splices length provided in the piers is sufficient to transfer forces between bars without sliding.

$$\tau_b = \frac{\tau_{bc}' r \left( \frac{S_b}{S_{bc}} \right)}{r - 1 + \left( \frac{S_b}{S_{bc}} \right) r} \quad (3.4)$$

$\tau_b$ : stress at the boundary,  $S_b$ : length of sliding,  $\tau'_{bc}$ : stress at the boundary between rebar and concrete  $\tau'_{bc} = \tau'_{b0} + 1.4f_l$ ,  $\tau'_{b0}$ : stress of boundary for rebars in the concrete core  $\tau'_{b0} = 20\sqrt{f'_c}/d_{bl} \leq 5.52$ ,  $f_l$ : pressure of confinement  $f_l = \alpha\rho_w f_{ym}$ ,  $S_{bc}$ : calibration parameter  $S_{bc} = S_{b0}(1 + \alpha f_l/f'_c)$ , with  $S_{b0}=0.25$  mm and  $\alpha=75$ ,  $r$ : calibration parameter,  $r = r_0 - k_r f_l/f'_c$  with  $r_0=2$  and  $k_r=13$ ,  $l_b$ , the boundary length,  $l_b = f_s d_{bl} / (4\tau_b)$ , where  $f_s = \sqrt{8\tau_b E_s S_b / d_{bl}}$  and  $d_{bl}$ : the diameter of longitudinal rebars

For the Warth bridge, for the different diameters of reinforcement, lap splices are sufficient.

**Table 3.2.** Lap splices analysis

	Lap splices available $l_s$	Boundary length $l_b$	$f_{sequiv}$
HA20	700mm	302 mm	545 MPa
HA16	560mm	267 mm	545 MPa
HA14	490mm	238 mm	545 MPa

## 4. PUSHOVER PRINCIPLES

In order to evaluate the seismic capacity of the Warth bridge, a pushover analysis was developed, according to the Eurocode 8 method. In order to well understand the behavior of the bridge, and to find the weak points, the pushover analysis was realized with hand calculation on Excel, step by step. First, the moment curvature curves were calculated for critical sections, considering the previous constitutive laws for materials. Then the behavior of the piers was estimated using force displacement curves. At least, the pushover analysis is done for the whole bridge, using Eurocode 8 spectrums. The

general principles of the analysis are summarized in the following figure.

Moreover, in this study, we supposed that the bottoms of the piers control the behavior. It is not really the case, because there is a brutal stop of the longitudinal bars between bottom sections and central sections, which creates the weak sections.

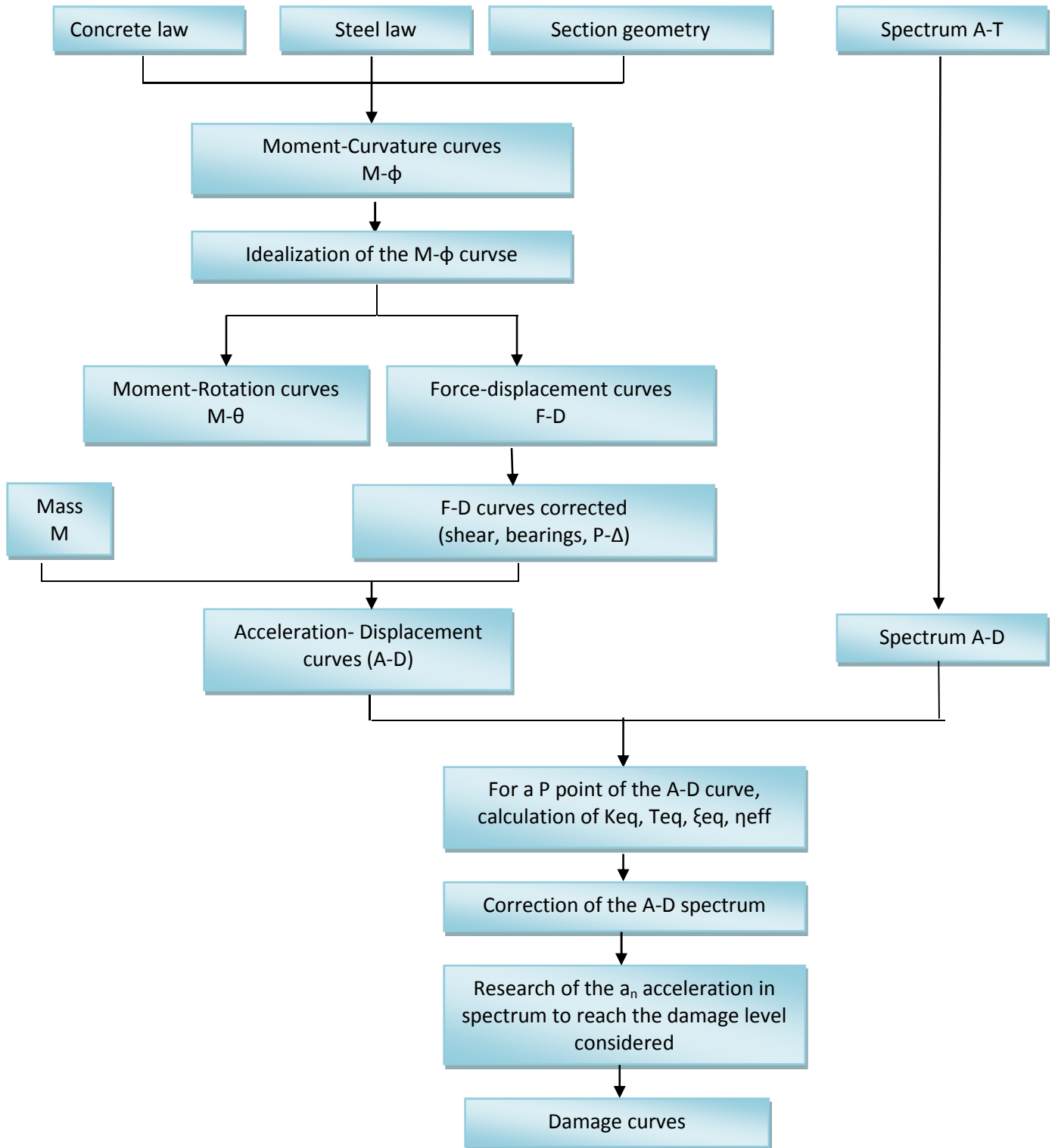


**Figure 7.** Pushover analysis developed with hand calculation

## 5. RESULTS

### 5.1. Moment-curvature curves

The moment curvature curves were determined using the previous constitutive laws corrected to take into account no-conform detailing. For A40 and A70 piers, we obtained the following results:

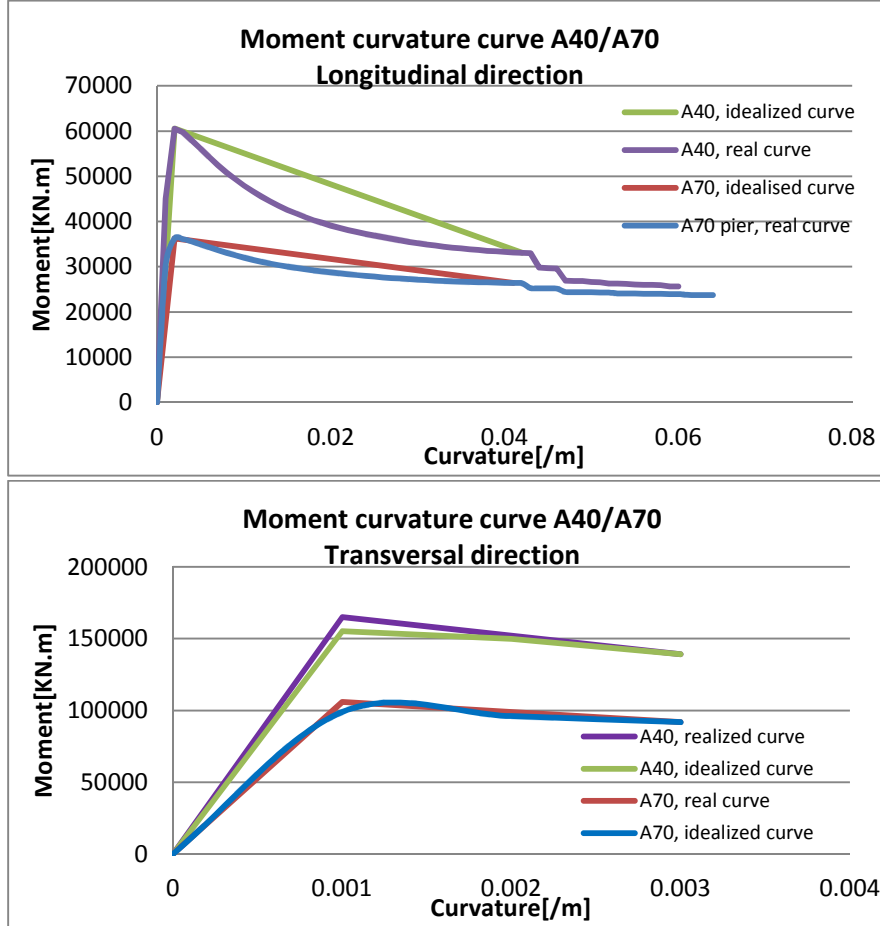


**Figure 8.** Moment curvature curves for A40 and A70 piers in longitudinal and transversal direction

As it can be observed, moment curvature curves are very unfavorable, because of the buckling consideration for steel, and because, for simplification in calculation, compressive law for steel has been considered for compression and tension in reinforcement. Nevertheless, as the curve is considered to be stopped when 20% of the capacity is lost, this phenomenon is weakened for the rest of the calculation.

### 5.2. Force displacement curves

The Eurocode 8 relations were used to calculate the force displacement curves from the moment curvature ones, using the following parameters:

$$\text{Elastic displacement } d_y = \phi_y H^2 / 3 \quad (5.1)$$

$$\text{Ultimate displacement } d_u = d_y + d_{p,u} = \phi_y H^2 / 3 + (\phi_u - \phi_y) L_p (H - 0.5 L_p) \lambda (\alpha_s) \quad (5.2)$$

$$\text{Elastic strength } F_y = M_y / H \quad (5.3)$$

$$\text{Ultimate strength } F_u = M_u / H \quad (5.4)$$

Moreover force-displacement curves have to be corrected to take into account shear, elastomeric bearings and P-Delta effects. Shear is taken into account using Eurocode 8 formulas. Then, bearings are taken into account in force-displacement curves of the piers, considering the increase of

displacement they provide. Last, P-delta effect are taken into account using the 1st order theory :

$$F_{corrected} = F - \frac{P\Delta}{H} \quad ( 5.5)$$

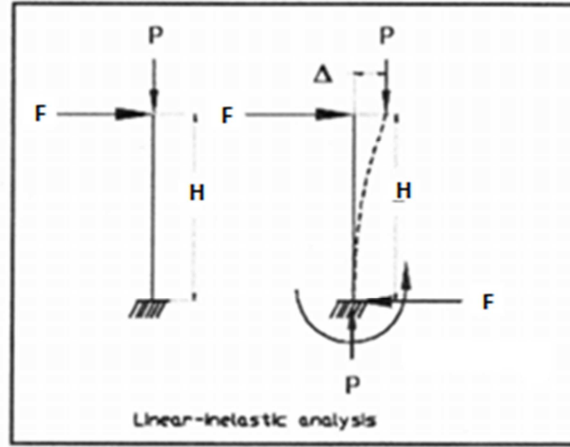


Figure 9. P-Delta theory

As a consequence, we obtained :

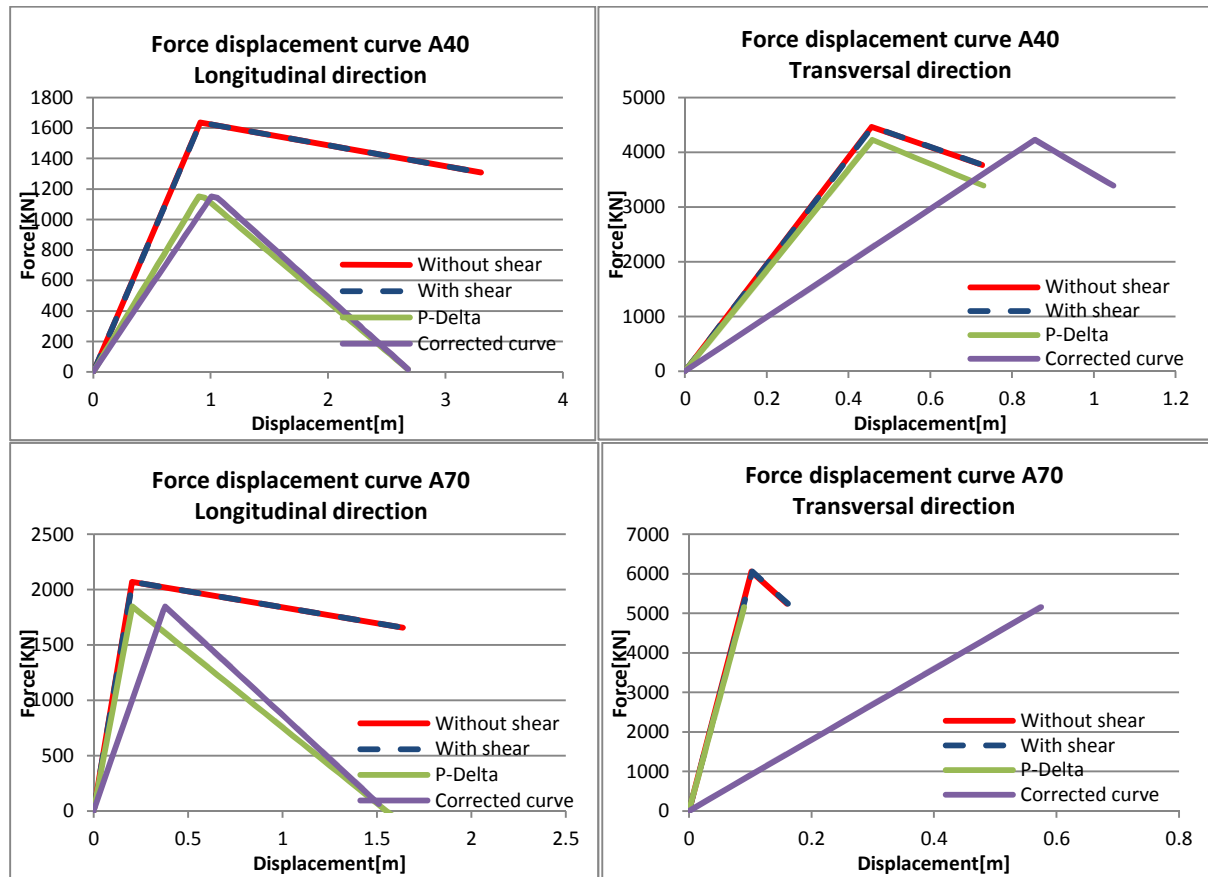
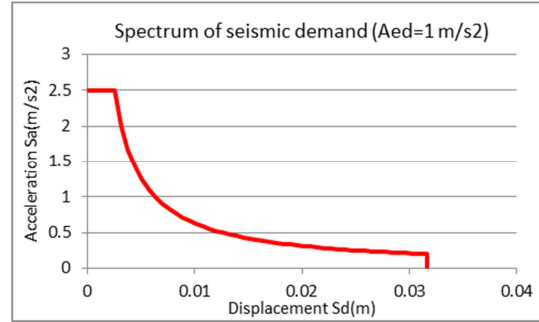


Figure 10. Force-displacement curves for A40 and A70 piers in longitudinal and transversal directions

For A40 piers, maximum displacements are very high, in particular in longitudinal direction. This is due to the fact, that for the present calculation, rotations have not been limited. Moreover, we can observe that in transversal direction, a large part of the displacement is given by the elastomeric bearings, whereas in longitudinal direction, as A40 pier is very flexible in longitudinal direction, the maximum displacement is provided by the pier. For A70 pier, conclusions are the same.

### 5.3. Damage curves

In order to realize the pushover analysis, the unitary spectrum of the Eurocode 8, was defined as following



**Figure 11.** Spectrum from Eurocode 8-1

Then, for all points of the capacity curve of the bridge, following characteristics shall be calculated:

$$\text{Secant equivalent rigidity } K_{eq} = F_p / d_p \quad (5.6)$$

$$\text{Equivalent period: } T_{eq} = 2\pi \sqrt{M_{eq} / K_{eq}} \quad (5.7)$$

$$\text{Ductility } \mu = d / d_y \quad (5.8)$$

$$\text{Equivalent damping: } \xi_{eq} = 0.05 + \frac{1}{2\pi} \left( 1 - \frac{(1-0.03)}{\sqrt{\mu}} - 0.03\sqrt{\mu} \right) \quad (5.9)$$

This value is half the Takeda current value, due to the fact that for existing bridges, studies show that energy is only 2 or 3 times the one of the 1<sup>st</sup> cycle (Diagnostic et renforcement sismiques des ponts existants, Setra guideline).

After, the spectrum is corrected with the acceleration at each step to intersect the capacity curve of the bridge on a determined displacement. To modelize this complete analysis, a macro was done in Excel. For the whole bridge, we obtained the following curves:

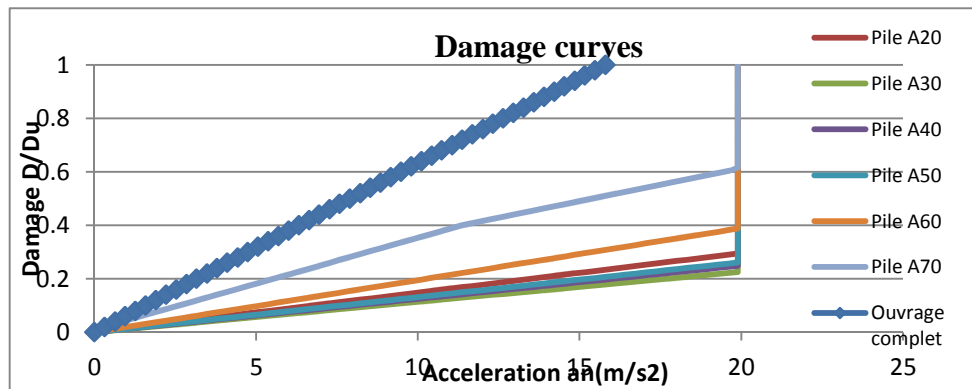


**Figure 12.** Damage curves for the whole bridge, longitudinal direction

As a consequence, we can observe that the rupture in longitudinal direction is obtained by collapse of the elastomeric bearings on abutments. Nevertheless, the collapse is obtained for a very important acceleration due to the important flexibility of the hollow core bridge piers in this direction.



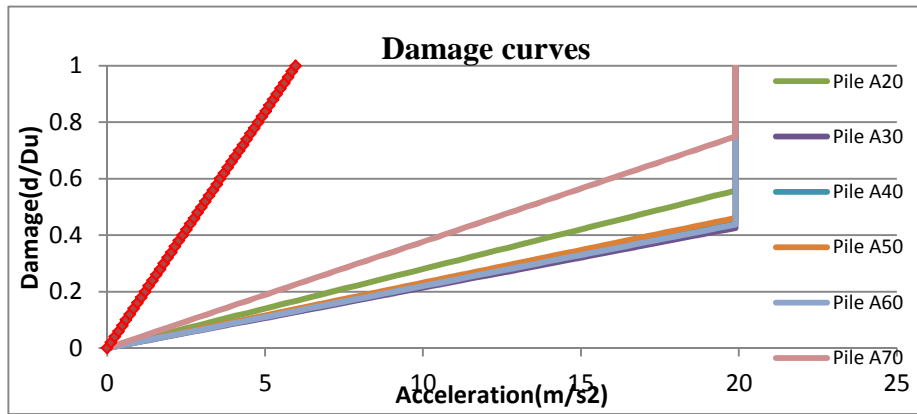


**Figure 13.** Damage curves for the whole bridge, transverse direction

In this case, the collapse is obtained for an acceleration of  $6\text{m/s}^2$  in the shortest pier, the A70 one.

## 6. COMPARISON WITH SOFISTIK SOFTWARE RESULTS

Results are obtained using second order theory calculation in Sofistik, using constitutive laws defined previously. For the A40 pier, we obtained the following results:

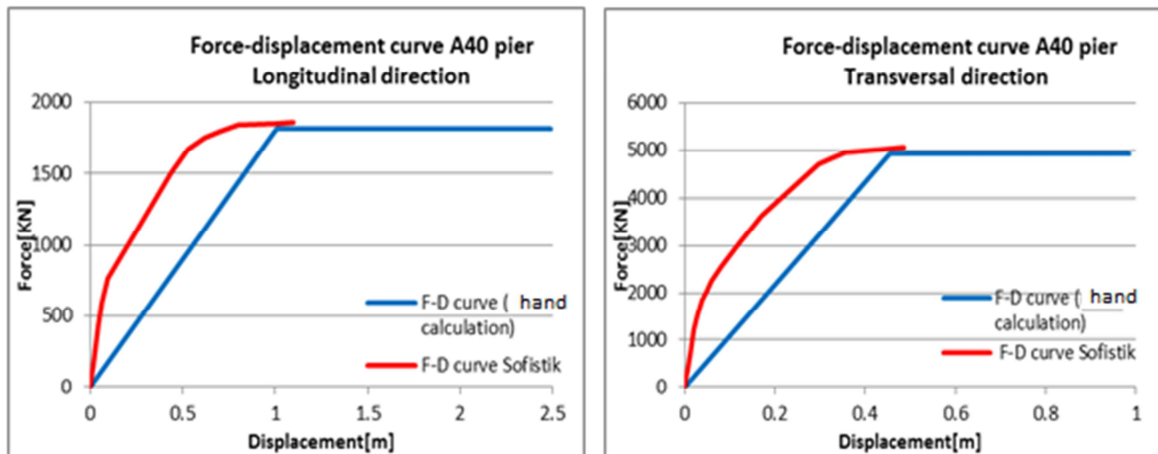


**Figure 14.** Comparison of Force Displacement curves from Sofistik analysis and hand calculation

We can observe several differences:

The difference of the initial stiffness is due to idealization of the moment-curvature curve done in hand calculation. In the case of the Warth bridge, we can note that this idealization is very important, this is because piers are cracking a lot thanks to their thin walls.

The ultimate displacement is very low in Sofistik calculation, this is due to an internal limitation on stresses on materials (0.6 on concrete and 0.75 on steel)

At least, the modelisation as a beam is not realistic because of the thickness of the wall, a modelisation with shell elements would have been better ( $e \ll b/8$ , Eurocode criterion for hollow core bridge piers).

## 7. CONCLUSION

We can conclude that the Warth bridge, regards to the hypothesis done on plastic hinge sections and elastomeric bearings free on abutments, has a great capacity under seismic solicitations ( $6\text{m/s}^2$  in the critical transversal direction).

Moreover this study permitted to develop pushover analysis tools and to better understand the real influence of parameters. In fact, this study put in light the important influence of idealization of the moment-curvature curves for high dimensions sections, as the hollow core bridge piers of the Warth

bridge. Moreover, for such structure, cracking is a very important parameter and the way to take it into account better shall be investigated, in order to affine the parameters for idealization. At least the method to take into account buckling shall be also affined, in order not to be so unfavorable. To conclude, the case of the Warth bridge was very interesting because with their specified piers shape, it permitted to put in light the limit of present pushover method with simplified modelisation, as described in Eurocode 8 and in literature.

## REFERENCES

- J.B. Mander, M.J.N. Priestley and R. Park, *Theoretical stress-strain model for confined concrete*, Journal of structural engineering V.114 No.8, 1988
- Augusto Gomes & Julio Appleton, *Nonlinear cyclic stress-strain relationship of reinforcing bars including buckling*, Engineering structure, 1997, vol 19
- Xiao et al (Y. Xiao, R. Ma (1997), *Seismic retrofit of RC circular columns using prefabricated composite jacketing*, Journal of structural engineering, March 1998
- Diagnostic et renforcement sismiques des ponts existants, Setra guideline.
- Eurocode 8 : Design of structures for earthquake resistance